



Structural stabilities and optical properties of $\text{Si}_x\text{Ge}_y\text{H}_z$ nanocrystals

Shao-Bin Qiu^a, Ya-Ting Wang^b, Chang-Chun He^a, Xiao-Lin Deng^a, Xiao-Bao Yang^{a,*}

^a Department of Physics, South China University of Technology, Guangzhou 510640, People's Republic of China

^b Guangdong Police College, Guangzhou 510230, People's Republic of China

ARTICLE INFO

Article history:

Received 27 February 2020
 Received in revised form 8 April 2020
 Accepted 20 May 2020
 Available online 1 June 2020
 Communicated by J.G. Lu

Keywords:

High-throughput first-principles calculations
 Structural recognition
 Structural stabilities
 Optical properties
 Nanocrystals

ABSTRACT

Based on the high-throughput first-principles calculations with structural recognition, we have systematically investigated the structural stabilities and optical properties of $\text{Si}_x\text{Ge}_y\text{H}_z$ nanocrystals (H-SiGeNCs), including various sizes, shapes and compositions. The total energies of H-SiGeNCs can be simply estimated by the bond energy model in high accuracy, where the error of test set is less than 0.5 meV per atom. According to the energy difference of Si/Ge in various bonding environments, we have determined the ground state structures by the geometry analysis, as is confirmed the convex hulls of formation enthalpy from the first-principles calculations. In addition, the energy gaps of H-SiGeNCs are modulated by the atomic distributions, as well as the vibrations of Si-H and Ge-H bonds at room temperature which is revealed by *ab initio* molecular dynamics simulations.

© 2020 Published by Elsevier B.V.

1. Introduction

Alloying is one of the most practical methods to tune the materials' properties and explore novel materials. Various metal alloys [1] and multi-component semiconductors [2–4] have been extensively studied. The order–disorder transition in the Cu–Au alloy has been the subject of numerous experimental and theoretical investigation [5], which is a typical system for studying the ordered structures of face-centered cubic lattice with nearest-neighbour interaction [6]. Multi-component semiconductors, $\text{Zn}_x\text{Mg}_{1-x}\text{S}_y\text{Se}_{1-y}$ and $(\text{GaN})_{1-x}(\text{ZnO})_x$, exhibit various electronic and optical properties, whose band structures can be effectively modulated by the concentrations and atomic distributions [2,4].

Due to the similar lattice constants in bulk Si and Ge, the $\text{Si}_x\text{Ge}_{1-x}$ alloys with the spontaneous ordering have been observed in epitaxially growth [7], which was proved to be the result of surface growth kinetics [8]. Various Si/Ge nanostructures, such as hetero-structures, quantum well structures, nanowires and nanocrystals, have been synthesised by self-assembling and self-ordering on single-crystal Si substrates [9], indicating potential applications of Si/Ge nanostructures such as photodetectors with improved performance or novel functionality. For example, the $\text{Si}_x\text{Ge}_{1-x}$ nanowires have been predicted to yield a direct band gap with an optically permitted transition [10,11].

Generally, the atomic distributions in alloy structures will evolve with environmental conditions, due to the free energies as a function of temperature. Combining the first-principles calculations with the cluster variation method, the phase diagram of semiconductor alloy can be obtained including the appearance of ordering and phase separation [12]. For example, the $\text{Si}_x\text{Ge}_{1-x}$ alloys in bulk are found to be a phase-separation system with a miscibility gap below 170 K [13]. Similarly, Monte-Carlo simulation has been further applied to the phase diagram of the CaO–MgO, Ti–Al, and Cu–Au systems [14], where the cluster expansion which has considered the effect of lattice vibrations will be in a better agreement with the experimental phase diagram [15].

With large surface/volume ratio, the chemical reactivity of metal nano-particles will be significantly enhanced, where the size and shape of stable structures will evolve as a function of thermal condition [16–18]. For example, the Pd–Rh nano-particles have been experimentally shown to be enriched in rhodium/palladium under oxidising/reducing conditions respectively [19], which has been confirmed by theoretical simulations [20]. For semiconductor quantumdots, the optical properties are dominated by the surface passivants due to the vibration effect, producing emission with a narrow full-width at half-maximum with high photo-luminescence quantum yield [21]. To simulate the optical adsorption spectrum, the first-principles calculations combined with importance sampling Monte Carlo methods is proposed, which is found to be in quantitative agreement with the experimental observation for diamondoids [22].

* Corresponding author.

E-mail address: scxbyang@scut.edu.cn (X.-B. Yang).

In this paper, we have theoretically investigated the hydrogen passivated SiGe nanocrystals (H-SiGeNCs), focusing on structural stabilities and optical properties. We have adopted a bond energy model for the total energies of $\text{Si}_x\text{Ge}_y\text{H}_z$, which is in good agreement with the results from the first-principles calculations. The test errors are lower than 0.5 meV per atom, and we have proposed a simple rule to determine the stable structures which are confirmed by the convex analysis of the formation enthalpy according to the first-principles calculations. The phase diagram of ground states can be correlated with the symmetry of H-SiGeNCs, where the sizes and atomic distributions can be tuned by the chemical potential of hydrogen passivants. Additionally, the energy gaps are found to be dominated by the sizes and atomic distributions. The vibration effect at room temperature is further studied based on *ab initio* molecular dynamics (AIMD) simulations.

2. Computational methods

Based on the density-functional theory (DFT) method implemented in the Vienna *ab initio* simulation package (VASP) [23,24], we have performed the first-principles calculations on H-SiGeNCs with various sizes, shapes, and Si/Ge composition. The generalised gradient approximation (GGA) functional [25,26] was employed for the exchange-correlation energy. The energy cut-off was set to be 500 eV and a mesh of $1 \times 1 \times 1$ in the Brillouin zone was used. All structures were fully relaxed by the conjugate gradient method and the forces on each atom were less than 0.01 eV/Å. The supercell was adopted with the vacuum distance larger than 10 Å to avoid the interactions caused by the periodical boundary condition. To consider the temperature effect, we have also used AIMD simulations at $T = 300$ K with the temperature controlled by a Nosé heat bath scheme [27].

The stable configurations of H-SiGeNCs can be determined by the convex hull analysis of formation enthalpy [28,29] as a function of Si or Ge atom number. The formation enthalpy is referred to pure nanocrystals with the same sizes and shapes, in which the number of H atoms remain the same. For a given H-SiGeNCs, the formation enthalpy $\Delta H(\text{Si}_x\text{Ge}_y\text{H}_z)$ is defined as:

$$\Delta H(\text{Si}_x\text{Ge}_y\text{H}_z) = E(\text{Si}_x\text{Ge}_y\text{H}_z) - [xE(\text{Si}_{x+y}\text{H}_z) + yE(\text{Ge}_{x+y}\text{H}_z)]$$

where $E(\text{Si}_x\text{Ge}_y\text{H}_z)$ and $E(\text{Si}_{x+y}\text{H}_z)/E(\text{Ge}_{x+y}\text{H}_z)$ are the total energies of the H-SiGeNCs and pure Si/Ge nanocrystals, respectively. The sign of the formation enthalpy indicates an exothermal or endothermic reaction compared to pure nanocrystals. The convex hull of formation enthalpy will indicate the ground state of H-SiGeNCs at 0 K.

As is known, it will be a challenge to search the stable structures due to the numerous candidates. To make an efficient screening, we have performed the structural recognition to prevent the repeated calculations of the same isomers, using the package of Structures of Alloys Generation And Recognition (SAGAR [30]). For example, there are 512 possible candidates for $\text{Si}_n\text{Ge}_{10-n}\text{H}_{16}$ while only 90 unique structures are found after the structural recognition. For $\text{Si}_n\text{Ge}_{14-n}\text{H}_{20}$, there are 1676 unique structures found in 16,384 possible candidates. The number of unique isomers will significantly grow as the size of H-SiGeNCs increases. In our previous studies [31–33], we have shown that the total energies of group-IV nanostructures ($X_m\text{H}_n$, $X = \text{C}, \text{Si}, \text{Ge}$) are dominated by the localized bonds of H-X and X-X, confirming the magic diamond nanocrystals observed experimentally ($\text{C}_{10}\text{H}_{16}$, $\text{C}_{14}\text{H}_{20}$, $\text{C}_{18}\text{H}_{24}$, $\text{C}_{22}\text{H}_{28}$ (1D), $\text{C}_{22}\text{H}_{28}$ (2D) and $\text{C}_{22}\text{H}_{28}$ (3D)) [34]. Thus, a fast and accurate estimation of energies for the H-SiGeNCs is necessary and important to screen stable structures.

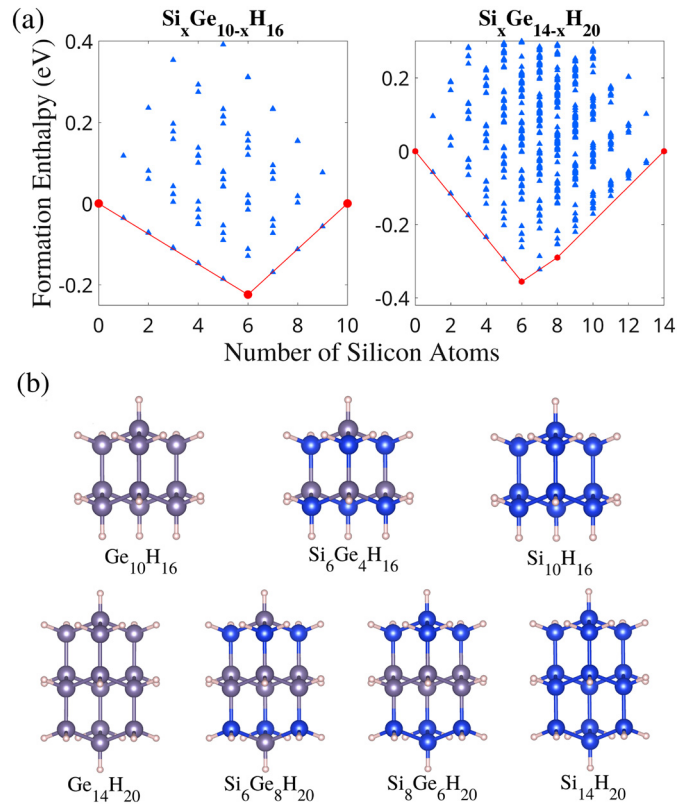


Fig. 1. Structural stabilities of $\text{Si}_x\text{Ge}_{10-x}\text{H}_{16}$ and $\text{Si}_x\text{Ge}_{14-x}\text{H}_{20}$. (a) Formation enthalpy of possible isomers is plot with blue triangles and the convex hull points are plot with red circles. (b) Stable structures according to the convex hull analysis, and blue/grey/white atoms are Si/Ge/H atoms, respectively. (For interpretation of the colours in the figure(s), the reader is referred to the web version of this article.)

3. Results

We have determined the ground state structures of H-SiGeNCs with various sizes, as shown in Sec. 3.1. The bond energy model is applied to describe the structural stabilities, demonstrating the evolution of stable structures. In Sec. 3.2, we consider the effect of chemical potential on the structural stabilities of H-SiGeNCs, where the energy gaps will vary with the distribution of Si/Ge atoms. The vibration effect on the gaps at room temperature is also discussed.

3.1. Bond energy model for H-SiGeNCs

According to the structural recognition, we have found 90 and 1676 unique isomers for $\text{Si}_x\text{Ge}_{10-x}\text{H}_{16}$ and $\text{Si}_x\text{Ge}_{14-x}\text{H}_{20}$, respectively. The total energies of all these structures were obtained by the DFT calculations. The convex hull analysis of formation enthalpy has been used to determine the stable structures of $\text{Si}_x\text{Ge}_{10-x}\text{H}_{16}$ and $\text{Si}_x\text{Ge}_{14-x}\text{H}_{20}$. As shown in Fig. 1(a), there is a stable structure of $\text{Si}_6\text{Ge}_4\text{H}_{16}$ for $\text{Si}_x\text{Ge}_{10-x}\text{H}_{16}$. Similarly, we have found two stable structures of $\text{Si}_6\text{Ge}_8\text{H}_{20}$ and $\text{Si}_8\text{Ge}_6\text{H}_{20}$ for $\text{Si}_x\text{Ge}_{14-x}\text{H}_{20}$, according to the convex hull analysis. Fig. 1(b) shows the stable structures of $\text{Si}_6\text{Ge}_4\text{H}_{16}$, $\text{Si}_6\text{Ge}_8\text{H}_{20}$ and $\text{Si}_8\text{Ge}_6\text{H}_{20}$. In $\text{Ge}_{10}\text{H}_{16}$, there are six dihydrides (GeH_2) and four monohydrides (GeH), and the most stable $\text{Si}_6\text{Ge}_4\text{H}_{16}$ is the structure with all GeH_2 replaced by SiH_2 . Similarly, $\text{Si}_6\text{Ge}_8\text{H}_{20}$ can be obtained from $\text{Ge}_{14}\text{H}_{20}$ by replacing all GeH_2 with SiH_2 . There are two kinds of GeH in $\text{Si}_6\text{Ge}_8\text{H}_{20}$, with one or three Si atoms as the nearest neighbours. The $\text{Si}_8\text{Ge}_6\text{H}_{20}$ is the structure with GeH replaced by SiH at the positions with three nearest neighbouring Si atoms. Thus, the ground state structures of H-SiGeNCs can be obtained from H-GeNCs by gradually replacing the Ge with Si based on the bonding configurations.

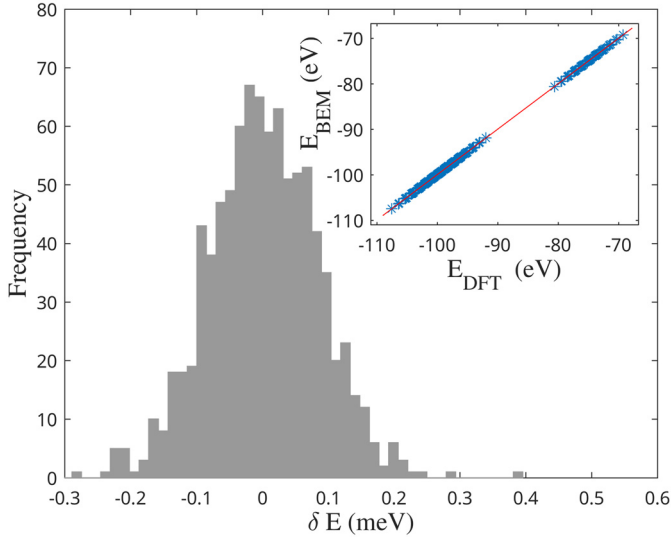


Fig. 2. Bond energy mode for H-SiGeNCs. The frequency shows the distribution of test errors (δE) for the total energies of $\text{Si}_x\text{Ge}_{10-x}\text{H}_{16}$ and $\text{Si}_x\text{Ge}_{14-x}\text{H}_{20}$. The inset shows the consistency of total energies between DFT and BEM.

Taking $\text{Si}_x\text{Ge}_{n-x}\text{H}_{n+6}$ ($n = 18, 22$) as examples, we have considered larger H-SiGeNCs with various sizes and shapes. The number of unique isomers are 68,352 for $\text{Si}_x\text{Ge}_{18-x}\text{H}_{24}$. The total number for $\text{Si}_x\text{Ge}_{22-x}\text{H}_{28}$ is 3,871,488, in which there are 1,065,984/2,098,176/707,328 isomers for 1D/2D/3D structures, respectively. In such cases, the total energies of all candidates using DFT will be over expensive. With the idea of bond energy model (BEM) [31], we estimate the energy with Si-H/Ge-H/Si-Si/Si-Ge/Ge-Ge bonds, where the parameters are fitted based on the DFT calculations of $\text{Si}_x\text{Ge}_{10-x}\text{H}_{16}$ and $\text{Si}_x\text{Ge}_{14-x}\text{H}_{20}$. As shown in Fig. 2, there is a linear dependence of energies from DFT and BEM (shown in the inset). Using 1,000 structures as the train set, we have found that the biggest deviation is less than 0.5 meV per atom for 776 test samples. In the fitting, we have used the energies from DFT calculations after full structural relaxation, which indicates that the structural stabilities of H-SiGeNCs can be excellently described by BEM.

The total energy of a given H-SiGeNCs is directly estimated based on BEM, and the analysis of parameters will bring insight of searching stable structures. For example, the energies of Si-Si/Si-Ge/Ge-Ge are $-2.244/-2.006/-1.788$ eV, respectively. Therefore, the phase separation will occur in the $\text{Si}_x\text{Ge}_{1-x}$ alloys at low temperature, as confirmed in previous studies [7,8]. In addition, the energies of Si-H and Ge-H are -3.355 eV and -2.985 eV, thus Si atom will be energetically preferable to aggregate towards surface, forming the core-shell structures. In the stable structures of $\text{Si}_6\text{Ge}_4\text{H}_{16}$, all Si atoms are bonded with two H atoms while the Ge atoms are bonded with one H atoms. It is reasonable that the energy of Si-H is 0.37 eV lower than that of Ge-H. Therefore, our BEM not only provides a fast and accurate estimation of energies, but also brings insight to understand the atomic distributions of stable structures.

3.2. Evolution of stable structures

The stable structures of H-SiGeNCs will vary with the sizes and shapes. Unfortunately, the number of possible candidates will grow exponentially as the sizes increase. According to BEM, we propose an analytical method to study the evolution of stable structures. In H-SiGeNCs, there are three types of bonding environment for Ge atoms: no H atom connected(A), one H atom connected(B) and two

Table 1

The energy difference of various sites replacing Ge atom with Si atom. The sites are distinguished by the number of H, Si, Ge atoms (α, β, γ).

Type	α, β, γ	ΔE (eV)
A1	0, 0, 4	-0.931
A2	0, 1, 3	-0.951
A3	0, 2, 2	-0.971
A4	0, 3, 1	-0.991
A5	0, 4, 0	-1.012
B1	1, 0, 3	-1.082
B2	1, 1, 2	-1.102
B3	1, 2, 1	-1.122
B4	1, 3, 0	-1.143
C1	2, 0, 2	-1.233
C2	2, 1, 1	-1.253
C3	2, 2, 0	-1.273

H atoms connected(C). The energy difference of the site replaced by Si atom is:

$$\Delta E = \alpha(E_{\text{Si-H}} - E_{\text{Ge-H}}) + \beta(E_{\text{Si-Si}} - E_{\text{Si-Ge}}) + \gamma(E_{\text{Si-Ge}} - E_{\text{Ge-Ge}})$$

where α, β and γ are the number of H, Si and Ge atoms at nearest neighbours, respectively.

Table 1 shows the energy difference for all possible cases of replacing Ge atom with Si atom, where ΔE is gradually decreased from A to C. When Ge atoms in H-GeNC are replaced by Si atoms one by one, the Si atoms will energetic-preferably replace the surface Ge atoms. To construct stable H-SiGeNCs, the GeH_2 will be firstly replaced by SiH_2 , where GeH will be further replaced by SiH when the Si concentration is increased. It is comprehensible because the bond energy of Si-H is much lower than the one of Ge-H bond. Inside H-SiGeNCs, Si atoms tend to aggregate together, where reducing the number of SiGe bonds will enhance the stabilities of H-SiGeNCs due to $E_{\text{Si-Si}} + E_{\text{Ge-Ge}} - 2E_{\text{Si-Ge}} < 0$. Therefore, the ground state structures of H-SiGeNCs can be obtained by the analysis of local geometry, gradually replacing Ge atoms in H-GeNCs with Si atoms.

Taking the $\text{Ge}_{10}\text{H}_{16}$ as an example, there are two isomers of $\text{SiGe}_9\text{H}_{16}$ and the one with C1 kind of Ge replaced by Si is more stable. From $\text{SiGe}_9\text{H}_{16}$ to $\text{Si}_6\text{Ge}_4\text{H}_{16}$, the lowest formation enthalpy for given concentration decrease linearly with the number of Si atoms. Then, there are four Ge atoms of B4 kind and the lowest formation enthalpy will increase when the number of Si atoms further increases. As a result, $\text{Si}_6\text{Ge}_4\text{H}_{16}$ is a ground state structure corresponding to the convex point of formation enthalpy. For $\text{Ge}_{14}\text{H}_{20}$, $\text{Si}_6\text{Ge}_8\text{H}_{20}$ is one ground state structure with six Ge atoms of C1 kind replaced by Si. There are two Ge atoms of B4 and six of B2 respectively, where ΔE of B4 is lower than that of B2. Thus, $\text{Si}_8\text{Ge}_6\text{H}_{20}$ is another ground state structure as confirmed in Fig. 1. Similarly, $\text{Si}_7\text{Ge}_{11}\text{H}_{24}$ is one ground state structure of $\text{Si}_x\text{Ge}_{18-x}\text{H}_{24}$ due to seven Ge atoms of C1 in $\text{Ge}_{18}\text{H}_{24}$. $\text{Si}_9\text{Ge}_9\text{H}_{24}$ and $\text{Si}_{17}\text{Ge}_1\text{H}_{24}$ are stable (as shown in Fig. 3(a)) as there are two/eight Ge atoms of B4/B2 kind, respectively. There is a Ge atom of A5 kind and the slope of the lowest formation enthalpy changes at $\text{Si}_{17}\text{Ge}_1\text{H}_{24}$.

There are three isomers of $\text{Ge}_{22}\text{H}_{28}$, 1D, 2D and 3D [34]. There are eight Ge atoms of C1 and $\text{Si}_8\text{Ge}_{14}\text{H}_{28}$ is stable for 1D $\text{Si}_x\text{Ge}_{22-x}\text{H}_{28}$. Due to two/ten Ge atoms of B4/B2, $\text{Si}_{10}\text{Ge}_{12}\text{H}_{28}$ and $\text{Si}_{20}\text{Ge}_2\text{H}_{28}$ are also stable. Similarly, $\text{Si}_8\text{Ge}_{14}\text{H}_{28}$, $\text{Si}_{10}\text{Ge}_{12}\text{H}_{28}$ and $\text{Si}_{20}\text{Ge}_2\text{H}_{28}$ are stable for 2D $\text{Si}_x\text{Ge}_{22-x}\text{H}_{28}$. For $\text{Ge}_{22}\text{H}_{28}$ with 3D geometry, $\text{Si}_9\text{Ge}_{13}\text{H}_{28}$ is one ground state structure due to nine Ge atoms of C1. $\text{Si}_{12}\text{Ge}_{10}\text{H}_{28}$ and $\text{Si}_{18}\text{Ge}_4\text{H}_{28}$ are stable as there are

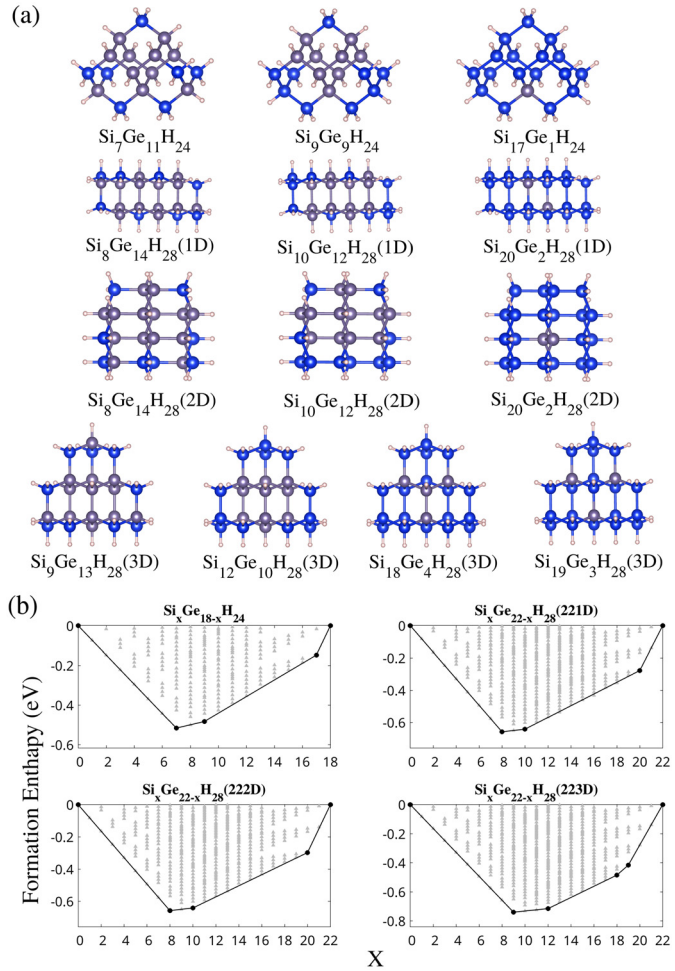


Fig. 3. Structural stabilities for various H-SiGeNCs. (a) Stable structures of $\text{Si}_x\text{Ge}_{18-x}\text{H}_{24}$ and $\text{Si}_x\text{Ge}_{22-x}\text{H}_{28}$ with various shapes; (b) Formation enthalpy and convex hull of $\text{Si}_x\text{Ge}_{18-x}\text{H}_{24}$ and $\text{Si}_x\text{Ge}_{22-x}\text{H}_{28}$ with various shapes.

three/six Ge atoms of B4/B2 kind, respectively. In $\text{Si}_{18}\text{Ge}_4\text{H}_{28}$, there are one/three Ge atoms of B1/A4, respectively. $\text{Si}_{19}\text{Ge}_3\text{H}_{28}$ is found to be more stable as ΔE of B1 is lower than that of A4. Therefore, we can find the ground state structure of H-SiGeNCs based on the symmetry analysis of the geometry, which are shown in Fig. 3(a) for details.

To verify the stable structures of H-SiGeNCs, we have obtained the formation enthalpy as a function of the number of Si atoms, where the total energies of all unique isomers are calculated by BEM. As shown in Fig. 3(b), the convex hull analysis shows that there are three stable structures for $\text{Si}_x\text{Ge}_{18-x}\text{H}_{24}$, which are $\text{Si}_7\text{Ge}_{11}\text{H}_{24}$, $\text{Si}_9\text{Ge}_9\text{H}_{24}$, and $\text{Si}_{17}\text{Ge}_1\text{H}_{24}$ (shown in Fig. 3(a)). Similarly, $\text{Si}_8\text{Ge}_{14}\text{H}_{28}$, $\text{Si}_{10}\text{Ge}_{12}\text{H}_{28}$, and $\text{Si}_{20}\text{Ge}_2\text{H}_{28}$ are stable structures for $\text{Si}_x\text{Ge}_{22-x}\text{H}_{28}$ (1D/2D). There are four stable structures for $\text{Si}_x\text{Ge}_{22-x}\text{H}_{28}$ (3D): $\text{Si}_9\text{Ge}_{13}\text{H}_{28}$, $\text{Si}_{12}\text{Ge}_{10}\text{H}_{28}$, $\text{Si}_{18}\text{Ge}_4\text{H}_{28}$, and $\text{Si}_{19}\text{Ge}_3\text{H}_{28}$. Thus, we have determined the stable structures of H-SiGeNCs with various sizes and shapes.

In our previous study [33], we have found that the hydrogen passivants would modulate the shape of silicon-carbide nanocrystals. Note that Si and C atoms are arranged orderly in silicon-carbide nanocrystals, while Si and Ge atoms will mix randomly in H-SiGeNCs. To describe the structural stabilities, the Gibbs free energy difference (ΔG) is defined as a function of chemical potential of Si/Ge/H ($\mu_{\text{Si}}/\mu_{\text{Ge}}/\mu_{\text{H}}$):

$$\Delta G = \frac{E - x\mu_{\text{Si}} - y\mu_{\text{Ge}} - z\mu_{\text{H}}}{x + y + z}$$

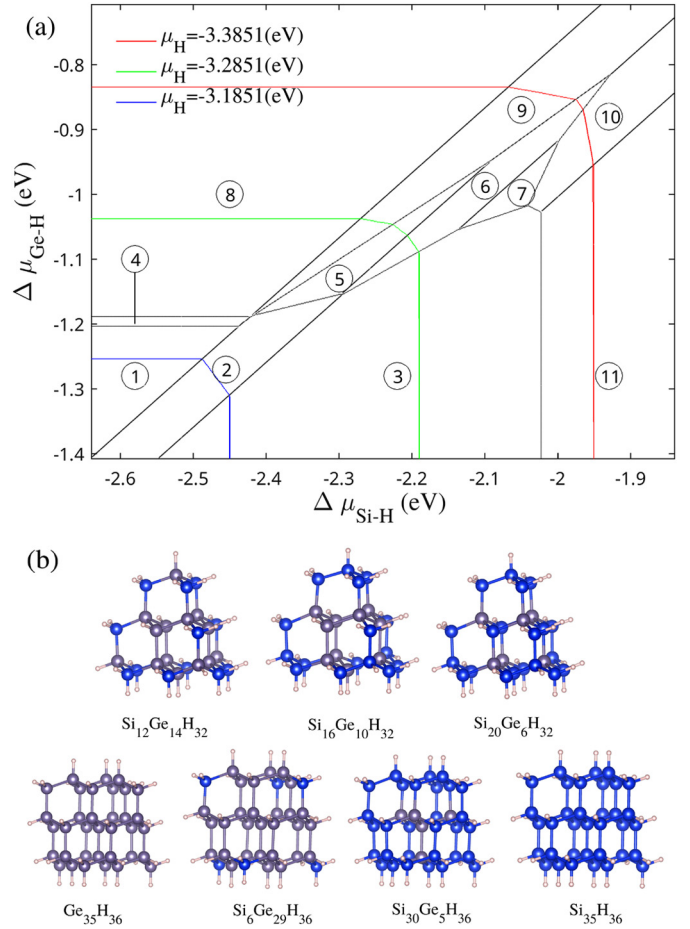


Fig. 4. Ground state structures for H-SiGeNCs as a function of chemical potential. (a) Phase diagram; (b) Ground state structures: ① $\text{Ge}_{10}\text{H}_{16}$ ② $\text{Si}_6\text{Ge}_4\text{H}_{16}$ ③ $\text{Si}_{10}\text{H}_{16}$ ④ $\text{Ge}_{14}\text{H}_{20}$ ⑤ $\text{Si}_{12}\text{Ge}_{14}\text{H}_{32}$ ⑥ $\text{Si}_{16}\text{Ge}_{10}\text{H}_{32}$ ⑦ $\text{Si}_{20}\text{Ge}_6\text{H}_{32}$ ⑧ $\text{Ge}_{35}\text{H}_{36}$ ⑨ $\text{Si}_6\text{Ge}_{29}\text{H}_{36}$ ⑩ $\text{Si}_{30}\text{Ge}_5\text{H}_{36}$ ⑪ $\text{Si}_{35}\text{H}_{36}$.

$$\begin{aligned} &= \frac{E - x(\mu_{\text{Si}} - \mu_{\text{H}}) - y(\mu_{\text{Ge}} - \mu_{\text{H}}) - (x + y + z)\mu_{\text{H}}}{x + y + z} \\ &= \frac{E - x\Delta\mu_{\text{Si-H}} - y\Delta\mu_{\text{Ge-H}}}{x + y + z} - \mu_{\text{H}} \end{aligned}$$

Here ΔG is found to be dominated by $\Delta\mu_{\text{Si-H}}$ and $\Delta\mu_{\text{Ge-H}}$, which are the relative potentials of μ_{Si} and μ_{Ge} compared to μ_{H} . However, the value of hydrogen chemical potential will affect the sign of ΔG , corresponding to an exothermic or endothermic reaction.

As shown in Fig. 4(a), we have determined the structural evolution as a function of $\Delta\mu_{\text{Si-H}}$ and $\Delta\mu_{\text{Ge-H}}$. With three given values of μ_{H} , the phase diagram remains the same and the boundaries between an exothermic or endothermic reaction are shown. As μ_{H} increases, more reactions will be exothermic and the structures in the phase diagram will be more stable.

Fig. 4(b) demonstrates the detailed structures found in the phase diagram of ground state. Besides the structures of $\text{Si}_x\text{Ge}_{n-x}\text{H}_{n+6}$ ($n = 10, 14, 18, 22$), we have also considered another two typical H-SiGeNCs ($\text{Si}_x\text{Ge}_{26-x}\text{H}_{32}$ and $\text{Si}_x\text{Ge}_{35-x}\text{H}_{36}$) with the symmetry of tetrahedral and octahedron. Under low $\Delta\mu_{\text{Si-H}}$ and $\Delta\mu_{\text{Ge-H}}$, $\text{Ge}_{10}\text{H}_{16}$, $\text{Si}_6\text{Ge}_4\text{H}_{16}$ and $\text{Si}_{10}\text{H}_{16}$ are stable, which are the ground state structures of $\text{Si}_x\text{Ge}_{10-x}\text{H}_{16}$. As $\Delta\mu_{\text{Si-H}}$ increases, $\text{Si}_{35}\text{H}_{36}$ with smaller H/Si ratio than $\text{Si}_{10}\text{H}_{16}$ will become more stable, and $\text{Ge}_{35}\text{H}_{36}$ will be also stable with the increasing of $\Delta\mu_{\text{Ge-H}}$. The stable structures found in $\text{Si}_x\text{Ge}_{26-x}\text{H}_{32}$ and $\text{Si}_x\text{Ge}_{35-x}\text{H}_{36}$ are also in agreement with our analytical method, in which Ge atoms are replaced by Si atoms following the C-B-A

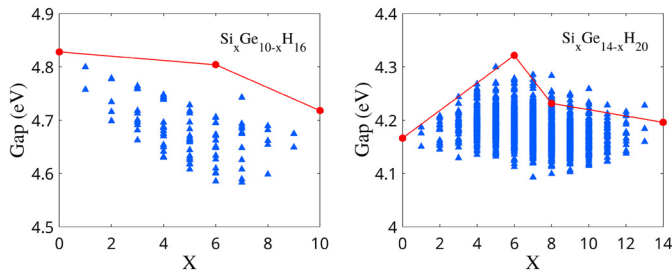


Fig. 5. Energy gap distributions of $\text{Si}_x\text{Ge}_{10-x}\text{H}_{16}$ and $\text{Si}_x\text{Ge}_{14-x}\text{H}_{20}$ as a function of Si/Ge compositions. Energy gaps of stable structures at $T = 0$ K are plotted in red for comparison.

sites as shown above. Therefore, the control of chemical potential will modulate the stable structures of H-SiGeNCs, which will further tune the optical properties. In our simulation, the sizes of H-SiGeNCs are quite smaller than those found in the previous experiments [35,36]. With the etching, Si nanocrystals have been reported to be with the size of 1 nm [37]. Further experimental attempts might be expected to confirm our theoretical predictions.

3.3. Optical properties

Combined with DFT calculations and BEM, we have systematically investigated the structural stabilities of H-SiGeNCs with various sizes and shapes. The energy difference of Si-H and Ge-H plays an important role to the formation enthalpy, providing a practical avenue to obtain the stable structures by the symmetry analysis. With different surface passivants, the energy difference of Si/Ge in various bonding environments (shown in Table 1) should be updated, and the stable structures of SiGe nanostructures can be obtained according to the similar analysis. Note that the convex hull analysis of formation enthalpy shows the stable structures will occur at $T = 0$ K, and there will be certain probabilities of occurrence for all the possible isomers at room temperature. For nanomaterials, the properties will be tuned by the sizes, attributed to the quantum confinement. In addition, the atomic distributions of Si/Ge are found to affect the energy gaps significantly.

Based on the DFT calculations, we have obtained the energy gaps of all possible candidates of $\text{Si}_x\text{Ge}_{10-x}\text{H}_{16}$ and $\text{Si}_x\text{Ge}_{14-x}\text{H}_{20}$ as shown in Fig. 5. The gaps of $\text{Si}_{10}\text{H}_{16}$ and $\text{Ge}_{10}\text{H}_{16}$ are 4.72/4.83 eV, respectively. Among the isomers of $\text{Si}_6\text{Ge}_4\text{H}_{16}$, the min/max gap is 4.59/4.80 eV, where the structure with max gap corresponds to the structure with lowest formation enthalpy. For the $\text{Si}_x\text{Ge}_{14-x}\text{H}_{20}$ isomers, the gaps of $\text{Si}_{14}\text{H}_{20}$ and $\text{Ge}_{14}\text{H}_{20}$ are 4.20/4.17 eV, respectively. Note that the max gap of $\text{Si}_6\text{Ge}_8\text{H}_{20}$ is 4.32 eV, which is the gap maximum for all $\text{Si}_x\text{Ge}_{14-x}\text{H}_{20}$ isomers. Among the $\text{Si}_6\text{Ge}_4\text{H}_{16}$ and $\text{Si}_6\text{Ge}_8\text{H}_{20}$ isomers, there is a general trend that the structures with more Si-H bonds will be more stable, corresponding to larger energy gaps. Thus, the distribution of Si-H and Ge-H bonds will affect the gaps of H-SiGeNCs.

In recent studies [21,22], the optical properties of nanomaterials are found to be dominated by the surface passivants and the vibration effect on the optical adsorption spectrum should be considered in theoretical simulation. We have performed the AIMD simulations to study the vibration effect at room temperature. For $\text{Si}_{10}\text{H}_{16}$, $\text{Ge}_{10}\text{H}_{16}$, and $\text{Si}_6\text{Ge}_4\text{H}_{16}$ isomers, we have simulated the systems at the temperature of 300 K with the time step of 1 fs. The energy gap distribution as a function of time is shown in Fig. 6(a). For $\text{Ge}_{10}\text{H}_{16}$, both HOMO and LUMO (shown in Fig. 6(b)) have a large oscillation and the oscillation is much smaller for $\text{Si}_{10}\text{H}_{16}$. Compared to $\text{Ge}_{10}\text{H}_{16}$, the broadening of gap distribution for $\text{Si}_{10}\text{H}_{16}$ is smaller, which indicates a sharper peak in the optical adsorption spectrum. We have analyzed the geometry effect on

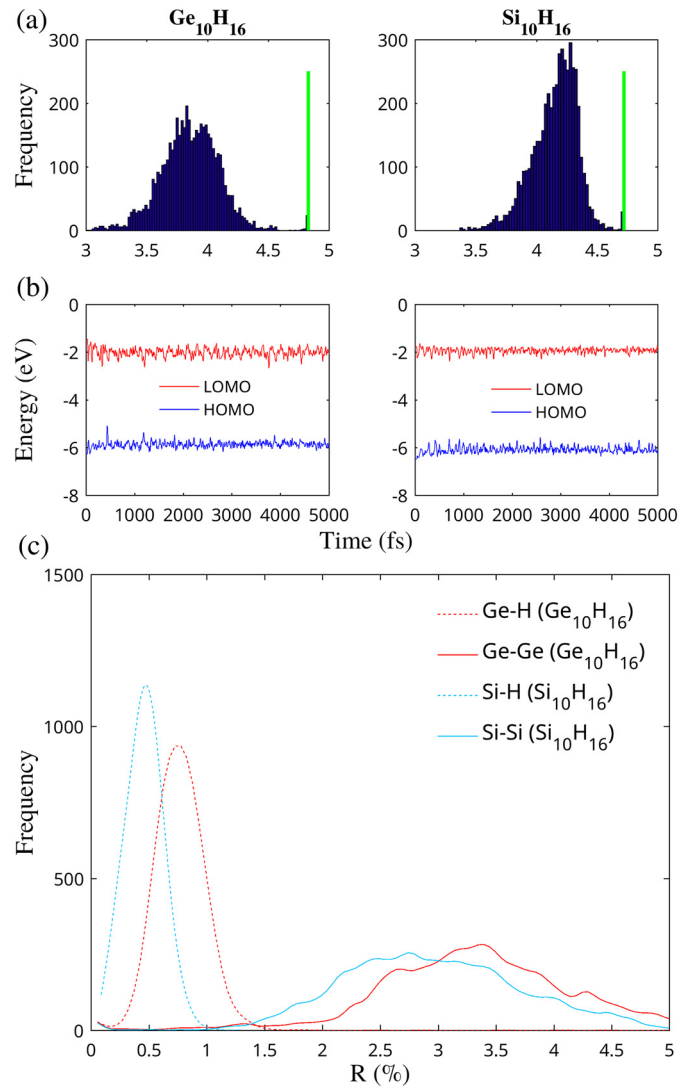


Fig. 6. The temperature effect on the optical properties: (a) The energy gap distributions in AIMD simulations. The gaps at $T = 0$ K are plotted with green lines; (b) the HOMO/LUMO energies variation in AIMD simulations; (c) The vibration of Si-H/Ge-H/Si-Si/Ge-Ge bonds compared to those at $T = 0$ K.

the gap distribution as shown in Fig. 6(c). The relative vibration of Ge-Ge bond is similar to that of Si-Si bond, while the one of Ge-H bond is almost twice of that for Si-H bond. The gap broadening of $\text{Si}_{10}\text{H}_{16}$ is also smaller than those of $\text{Si}_6\text{Ge}_4\text{H}_{16}$ isomers. Thus, the Ge-H bonds not only modulate the gap values of H-SiGeNCs, but also play an important role in the optical adsorption spectrum.

4. Conclusions

In summary, we have systematically investigated the structural stabilities and optical properties of H-SiGeNCs, based on the high-throughput first-principles calculations with structural recognition. We show that the total energies of H-SiGeNCs can be estimated by the bond energy model, which will enhance the screening of stable structures. The energy difference of Si-H and Ge-H plays an important role to the formation enthalpy, providing a practical avenue to obtain the stable structures by the symmetry analysis, as confirmed by the convex hulls of formation enthalpy from the first-principles calculations. The optical properties are found to be dominated by the vibration of Si-H and Ge-H bonds at room temperature.

Data availability statement

The data that support the findings of this study are available from the corresponding author upon reasonable request.

Declaration of competing interest

The authors declare that they have no known competing financial interests or personal relationships that could have appeared to influence the work reported in this paper.

Acknowledgements

This work was supported by Guangdong Natural Science Funds for Distinguished Young Scholars (No. 2014A030306024), National Natural Science Foundation of China (Nos. 11474100, U1601212), the Fundamental Research Funds for the Central Universities (No. 2018ZD46).

References

- [1] V. Ozolinš, C. Wolverton, A. Zunger, *Phys. Rev. B* 57 (1998) 6427.
- [2] A.M. Saitta, S. de Gironcoli, S. Baroni, *Phys. Rev. Lett.* 80 (1998) 4939.
- [3] Z. Xia, G. Liu, J. Wen, Z. Mei, M. Balasubramanian, M.S. Molokeev, L. Peng, L. Gu, D.J. Miller, Q. Liu, K.R. Poeppelmeier, *J. Am. Chem. Soc.* 138 (2016) 1158.
- [4] X. Xu, H. Jiang, *J. Chem. Phys.* 150 (2019) 034102.
- [5] B. Chakraborty, Z. Xi, *Phys. Rev. Lett.* 68 (1992) 2039.
- [6] K. Binder, *Phys. Rev. Lett.* 45 (1980) 811.
- [7] A. Ourmazd, J.C. Bean, *Phys. Rev. Lett.* 55 (1985) 765.
- [8] F.K. LeGoues, V.P. Kesan, S.S. Iyer, J. Tersoff, R. Tromp, *Phys. Rev. Lett.* 64 (1990) 2038.
- [9] K. Brunner, *Rep. Prog. Phys.* 65 (2001) 27.
- [10] X. Cartoixà, M. Palummo, H.I.T. Hauge, E.P.A.M. Bakkers, R. Rurali, *Nano Lett.* 17 (2017) 4753.
- [11] L. Zhang, M. d'Avezac, J.-W. Luo, A. Zunger, *Nano Lett.* 12 (2012) 984.
- [12] A.A. Mbaye, L.G. Ferreira, A. Zunger, *Phys. Rev. Lett.* 58 (1987) 49.
- [13] S. de Gironcoli, P. Giannozzi, S. Baroni, *Phys. Rev. Lett.* 66 (1991) 2116.
- [14] A. van de Walle, G. Ceder, *J. Phase Equilib.* 23 (2002) 348.
- [15] M. Klaseen, *Rev. Mod. Phys.* 74 (2002) 1221.
- [16] R. Ferrando, J. Jellinek, R.L. Johnston, *Chem. Rev.* 108 (2008) 845.
- [17] L.-L. Wang, T.L. Tan, D.D. Johnson, *Phys. Rev. B* 86 (2012) 035438.
- [18] F. Calvo, *Phys. Chem. Chem. Phys.* 17 (2015) 27922.
- [19] J.R. Renzas, W. Huang, Y. Zhang, M.E. Grass, D.T. Hoang, S. Alayoglu, D.R. Butcher, F.F. Tao, Z. Liu, G.A. Somorjai, *Phys. Chem. Chem. Phys.* 13 (2011) 2556.
- [20] L.-L. Wang, T.L. Tan, D.D. Johnson, *Nano Lett.* 14 (7077) (2014), PMID: 25411918.
- [21] F. Yuan, Y.-K. Wang, G. Sharma, Y. Dong, X. Zheng, P. Li, A. Johnston, G. Bappi, J. Fan, H. Kung, B. Chen, M. Saidaminov, K. Singh, O. Voznyy, O. Bakr, Z.-H. Lu, E. Sargent, *Nat. Photonics* 1 (2019).
- [22] C.E. Patrick, F. Giustino, *Nat. Commun.* 4 (2013) 2006.
- [23] G. Kresse, J. Furthmüller, *Phys. Rev. B* 54 (1996) 11169.
- [24] G. Kresse, D. Joubert, *Phys. Rev. B* 59 (1999) 1758.
- [25] J.P. Perdew, K. Burke, M. Ernzerhof, *Phys. Rev. Lett.* 77 (1996) 3865.
- [26] J.P. Perdew, K. Burke, M. Ernzerhof, *Phys. Rev. Lett.* 80 (1998) 891.
- [27] S. Nosé, *J. Chem. Phys.* 81 (1984) 511.
- [28] R. Arroyave, A. van de Walle, Z.-K. Liu, *Acta Mater.* 54 (2006) 473.
- [29] G. Trimarchi, A.J. Freeman, A. Zunger, *Phys. Rev. B* 80 (2009) 092101.
- [30] <http://sagar.compphys.cn/sagar>.
- [31] X. Yang, Y.-J. Zhao, H. Xu, B.I. Yakobson, *Phys. Rev. B* 83 (2011) 205314.
- [32] H. Lu, Y.-J. Zhao, X.-B. Yang, H. Xu, *Phys. Rev. B* 86 (2012) 085440.
- [33] Y.-T. Wang, Y.-J. Zhao, X.-B. Yang, *J. Phys. D, Appl. Phys.* 49 (2016) 245305.
- [34] Y.-T. Wang, Y.-J. Zhao, J.-H. Liao, X.-B. Yang, *J. Chem. Phys.* 148 (2018) 014306.
- [35] J.G. Zhu, C. White, J.D. Budai, S.P. Withrow, Y. Chen, *J. Appl. Phys.* 78 (1995) 4386.
- [36] G. Katsaros, P. Spathis, M. Stoffel, F. Fournel, M. Mongillo, V. Bouchiat, F. Lefloch, A. Rastelli, O.G. Schmidt, S. De Franceschi, *Nat. Nanotechnol.* 5 (2010) 458.
- [37] G. Belomoin, J. Therrien, A. Smith, S. Rao, R. Twisten, S. Chaieb, M.H. Nayfeh, L. Wagner, *L. Mitas, Appl. Phys. Lett.* 80 (2002) 841.